Dielectric nanostructures for broadband light trapping in organic solar cells

Aaswath Raman, Zongfu Yu, and Shanhui Fan*

Ginzton Laboratory, Stanford University, Stanford, California 94305, USA

*shanhui@stanford.edu

Abstract: Organic bulk heterojunction solar cells are a promising candidate for low-cost next-generation photovoltaic systems. However, carrier extraction limitations necessitate thin active layers that sacrifice absorption for internal quantum efficiency or vice versa. Motivated by recent theoretical developments, we show that dielectric wavelength-scale grating structures can produce significant absorption resonances in a realistic organic cell architecture. We numerically demonstrate that 1D, 2D and multi-level ITO-air gratings lying on top of the organic solar cell stack produce a 8-15% increase in photocurrent for a model organic solar cell where PCDTBT:$PC_{71}BM$ is the organic semiconductor. Specific to this approach, the active layer itself remains untouched yet receives the benefit of light trapping by nanostructuring the top surface below which it lies. The techniques developed here are broadly applicable to organic semiconductors in general, and enable partial decoupling between active layer thickness and photocurrent generation.

OCIS codes: (350.6050) Solar energy; (350.4238) Nanophotonics and photonic crystals; (050.0050) Diffraction and gratings.

References and links

1. H. Hoppe and N. S. Sariciftci, "Organic solar cells: An overview," J. Mater. Res. **19**, 1924–1945 (2004).
2. A. C. Mayer, S. R. Scully, B. E. Hardin, M. W. Rowell, and M. D. McGehee, "Polymer-based solar cells," Mater. Today **10**, 28–33 (2007).
3. D. Muhlbacher, M. Scharber, M. Morana, Z. Zhu, D. Waller, R. Gaudiana, and C. Brabec, "High photovoltaic performance of a low-bandgap polymer," Adv. Mater. **18**, 2884–2889 (2006).
4. S. H. Park, A. Roy, S. Beaupr, S. Cho, N. Coates, J. S. Moon, D. Moses, M. Leclerc, K. Lee, and A. J. Heeger, "Bulk heterojunction solar cells with internal quantum efficiency approaching 100%," Nat. Photonics **3**, 297–302 (2009).
5. J. Kim, S. Kim, H.-H. Lee, K. Lee, W. Ma, X. Gong, and A. Heeger, "New architecture for high-efficiency polymer photovoltaic cells using solution-based titanium oxide as an optical spacer," Adv. Mater. **18**, 572–576 (2006).
6. A. Hayakawa, O. Yoshikawa, T. Fujieda, K. Uehara, and S. Yoshikawa, "High performance polythiophene/fullerene bulk-heterojunction solar cell with a tiox hole blocking layer," Appl. Phys. Lett. **90**, 163517 (2007).
7. S.-B. Rim, S. Zhao, S. R. Scully, M. D. McGehee, and P. Peumans, "An effective light trapping configuration for thin-film solar cells," Appl. Phys. Lett. **91**, 243501 (2007).
8. M. Niggemann, M. Glatthaar, A. Gombert, A. Hinsch, and V. Wittwer, "Diffraction gratings and buried nano-electrodes–architectures for organic solar cells," Thin Solid Films **451-452**, 619–623 (2004).
9. S.-I. Na, S.-S. Kim, J. Jo, S.-H. Oh, J. Kim, and D.-Y. Kim, "Efficient polymer solar cells with surface relief gratings fabricated by simple soft lithography," Adv. Func. Mater. **18**, 3956–3963 (2008).
10. J. R. Tumbleston, D.-H. Ko, E. T. Samulski, and R. Lopez, "Absorption and quasiguided mode analysis of organic solar cells with photonic crystal photoactive layers," Opt. Express **17**, 7670–7681 (2009).

#147585 - $15.00 USD Received 26 May 2011; revised 29 Jun 2011; accepted 1 Jul 2011; published 15 Sep 2011

11. D.-H. Ko, J. R. Tumbleston, L. Zhang, S. Williams, J. M. DeSimone, R. Lopez, and E. T. Samulski, "Photonic crystal geometry for organic solar cells," Nano Lett. **9**, 2742–2746 (2009).
12. E. Yablonovitch, "Statistical ray optics," J. Opt. Soc. Am. **72**, 899–907 (1982).
13. Z. Yu, A. Raman, and S. Fan, "Fundamental limit of light trapping in grating structures," Opt. Express **18**, A366–A380 (2010).
14. H. R. Stuart and D. G. Hall, "Thermodynamic limit to light trapping in thin planar structures," J. Opt. Soc. Am. A **14**, 3001–3008 (1997).
15. Z. Yu, A. Raman, and S. Fan, "Fundamental limit of nanophotonic light trapping in solar cells," Proc. Natl. Acad. Sci. **107**, 17491–17496 (2010).
16. N. C. Lindquist, W. A. Luhman, S.-H. Oh, and R. J. Holmes, "Plasmonic nanocavity arrays for enhanced efficiency in organic photovoltaic cells," Appl. Phys. Lett. **93**, 123308 (2008).
17. H. Shen, P. Bienstman, and B. Maes, "Plasmonic absorption enhancement in organic solar cells with thin active layers," J. Appl. Phys. **106**, 073109 (2009).
18. C. Min, J. Li, G. Veronis, J.-Y. Lee, S. Fan, and P. Peumans, "Enhancement of optical absorption in thin-film organic solar cells through the excitation of plasmonic modes in metallic gratings," Appl. Phys. Lett. **96**, 133302 (2010).
19. D. M. Whittaker and I. S. Culshaw, "Scattering-matrix treatment of patterned multilayer photonic structures," Phys. Rev. B **60**, 2610–2618 (1999).
20. S. G. Tikhodeev, A. L. Yablonskii, E. A. Muljarov, N. A. Gippius, and T. Ishihara, "Quasiguided modes and optical properties of photonic crystal slabs," Phys. Rev. B **66**, 045102 (2002).
21. C. Brabec, V. Dyakonov, and U. Scherf, *Organic Photovoltaics: Materials, Device Physics, and Manufacturing Technologies* (Wiley-VCH, 2008).
22. S. B. Mallick, M. Agrawal, and P. Peumans, "Optimal light trapping in ultra-thin photonic crystal crystalline silicon solar cells," Opt. Express **18**, 5691–5706 (2010).
23. V. Shrotriya, G. Li, Y. Yao, C.-W. Chu, and Y. Yang, "Transition metal oxides as the buffer layer for polymer photovoltaic cells," Appl. Phys. Lett. **88**, 073508 (2006).
24. M. D. Irwin, D. B. Buchholz, A. W. Hains, R. P. H. Chang, and T. J. Marks, "p-type semiconducting nickel oxide as an efficiency-enhancing anode interfacial layer in polymer bulk-heterojunction solar cells," Proc. Natl. Acad. Sci. U.S.A. **105**, 2783–2787 (2008).
25. H. Wu, L. Hu, T. Carney, Z. Ruan, D. Kong, Z. Yu, Y. Yao, J. J. Cha, J. Zhu, S. Fan, and Y. Cui, "Low reflectivity and high flexibility of tin-doped indium oxide nanofiber transparent electrodes," J. Am. Chem. Soc. **133**, 27–29 (2011).
26. K.-Y. Yang, K.-M. Yoon, S. Lim, and H. Lee, "Direct indium tin oxide patterning using thermal nanoimprint lithography for highly efficient optoelectronic devices," J. Vac. Sci. Technol. B **27**, 2786–2789 (2009).

1. Introduction

A major thrust of current photovoltaics research is to find ways of reducing the cost of solar cells to make them competitive with existing grid-scale energy sources. To this end there has been a remarkable flourishing of research into new photovoltaic materials that lend themselves to low-cost manufacturing processes. Organic photovoltaics (OPV) in particular has taken off with the promise of low materials costs and fast, scalable manufacturing [1–3].

However, an important factor limiting the efficiency of current OPV cells is the length-scale mismatch between the electronic carrier extraction, and optical absorption of the organic semiconductors used. While organic semiconductors are typically strong optical absorbers, it is difficult to efficiently extract photo-generated charge carriers from them. For example, in solar cells using recently developed organic bulk heterojunctions, the active layer needs to have a thickness of less than 100 nm for efficient carrier extraction [4]. These thin layers leave many photons unharvested, and have thus motivated much recent interest in optical design and light trapping [5–11] for organic solar cells.

Light trapping encompasses an array of techniques designed to enhance photon absorption in a solar cell. In thick crystalline silicon solar cells, light trapping can be described by a ray optics picture in terms of the enhancement of optical path length inside the cell. For cells that are many wavelengths thick, the ray optics theory of light trapping derived a limit of $4n^2$ to the absorption enhancement that one could maximally obtain [12]. This limit in fact still applies when the cell's thickness is more than about half a wavelength thick [13, 14], and hence applies

#147585 - $15.00 USD Received 26 May 2011; revised 29 Jun 2011; accepted 1 Jul 2011; published 15 Sep 2011

to many recent works on light trapping in inorganic cells. In contrast to most inorganic cells, the active layers in organic cells have thicknesses that are far smaller than the wavelength, thereby placing them in the nanophotonic regime. Recently, we showed that the 'conventional' $4n^2$ limit on light trapping could be substantially surpassed in this nanophotonic regime [13, 15]. The theory in [13, 15] moreover offers new directions and ideas relevant to light trapping for thin active layers, which we pursue in this paper.

Recent work on light trapping for organic solar cells has used metallic nanostructures [16–18], or structured the active layer itself as a grating or photonic crystal [10, 11]. Both of these approaches can present implementation challenges. The use of metallic nanostructures has the tendency to increase parasitic optical absorption loss due to the metal, which competes with absorption in the active layer. Structuring the active layer can be challenging since the active layer is solution-processed and must retain a short path to electrical contacts for efficient charge carrier extraction.

Here we propose an alternative approach to light trapping in organic solar cells. Our approach leaves the active layer itself planar while altering the layers around it, and only uses low-loss dielectric components. We demonstrate that all-dielectric, top-surface one- and two-dimensional gratings can provide substantial broadband absorption enhancement in organic solar cells. In particular, we show that using ITO gratings on the top-surface we can scatter into ITO modes that provide absorption enhancement since the active layer is close to the ITO layer.

In Section 2, we introduce our model system where PCDTBT:$PC_{71}BM$ is used as the bulk heterojunction semiconductor. In Section 3, we theoretically motivate the choice of ITO gratings. In Section 4, we demonstrate that an optimized 1D ITO-air grating can produce broad absorption peaks that enhance polarization-averaged photocurrent by 8.31% relative to a reference planar cell with an active layer thickness of 35 nm. To overcome the issue of polarization-dependence we consider 2D ITO-air gratings in Section 5, which demonstrate 10.91% photocurrent enhancement. This enhancement can be increased up to 14.95% by reducing the thickness of the PEDOT:PSS layer. In Section 6, we briefly examine more sophisticated grating schemes that achieves light trapping through strong broadband scattering. We conclude in Section 7 by commenting on the viability of these designs and future directions for such light trapping schemes.

2. Materials and Methods

As a model system, we consider the cell structure shown in Fig. 1(a). The active layer is a 1:4 blend of PCDTBT:$PC_{71}BM$ spun from dichlorobenzene, as done in a recent paper which achieved a high efficiency of 6.1% for organic solar cells [4]. Currently, to achieve superior absorption it must be thicker (80-100 nm) than is ideal for current extraction. There is thus significant desire to achieve similar absorption for thinner layers of such organic semiconductors in general, in order to achieve higher internal quantum efficiency and overall power conversion efficiency. Materials above the active layer include PEDOT:PSS, and ITO, which together form the cell's top contact, and function as a relatively transparent conductor. Below the active layer is an optical spacer of TiOx (that also functionally acts a hole blocker) and finally a reflecting substrate of Ag. For all layers, refractive indices are either taken from tabulated values when available, or by our own fit to experimentally available ellipsometry and absorption data. Our simulations include both refractive indices and extinction coefficients, accounting for absorption in all layers.

Even though we consider this specific model system, we emphasize that the approach highlighted here is meant to be generally applicable to new bulk heterojunctions being developed and synthesized. Similar to PCDTBT:$PC_{71}BM$, these new organic semiconductors can achieve very high internal quantum efficiencies only in thinner layers (40-70 nm) than is ideal for ab-

#147585 - $15.00 USD Received 26 May 2011; revised 29 Jun 2011; accepted 1 Jul 2011; published 15 Sep 2011

sorption. The light trapping techniques we discuss in this paper can allow designers to keep active layers thin, which is beneficial for electronic reasons, while still retaining the overall absorption of a thicker layer.

The rigorous coupled wave analysis (RCWA) method is used to simulate and analyze the performance of candidate nanostructures. A scattering matrix implementation was used [19, 20], where the electromagnetic field in the spatial Fourier space for each layer is solved, and the scattering matrix of the whole structure is determined by matching boundary conditions between layers. For all structures considered in this paper, a square lattice is used. 10 Fourier orders sufficed to achieve convergence for both polarizations considered.

2.1. Optimized Planar Structure

To assess the performance of various structures we compare their performance against an optimized reference planar cell where the ITO layer is unstructured. The metric used to assess and optimize both the grating and planar cells' performance is the maximum achievable photocurrent density J_{max}, defined as

$$J_{max} = \int d\lambda \left[e \frac{\lambda}{hc} \frac{dI}{d\lambda} \alpha(\lambda) \right]. \tag{1}$$

In this expression $dI/d\lambda$ is the intensity of light incident on the solar cell per unit area and wavelength. In this paper we use the AM 1.5G spectrum (ASTM G173-03). $\alpha(\lambda)$ is the fraction of light absorbed by the active layer of the cell. We specifically integrate this over the spectrum relevant to this organic semiconductor, from 375 to 750 nm.

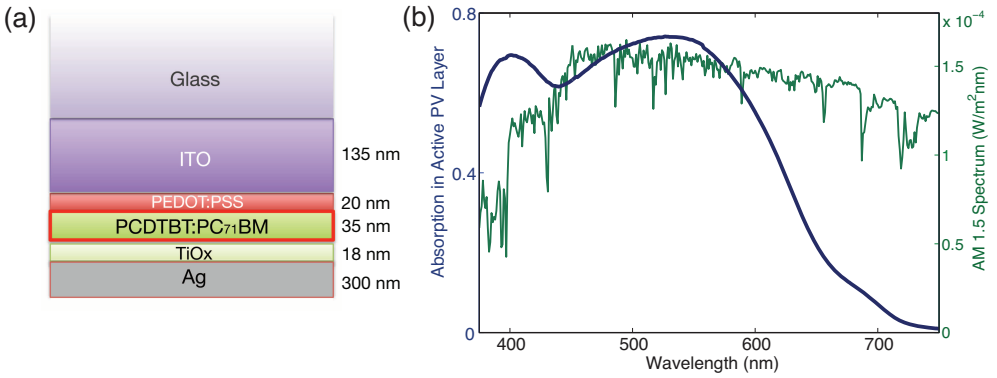

Fig. 1. (a) Schematic of the optimized planar reference cell, and (b) the absorption spectrum of the cell, with AM 1.5G spectrum also plotted for reference.

For most parts of the paper, the active PCDTBT:PC_{71}BM layer thickness is fixed to be 35 nm. This is deliberately thinner than active layers normally used in such OPV cells. Our aim is to highlight that with light trapping these thinner layers can achieve photocurrent generation on par with thicker cells.

For the planar structure shown in Fig. 1(a), an optimization is done for its ITO, and TiOx spacer layer thicknesses, resulting in heights of 135 nm, and 18 nm respectively. This optimized structure's absorption in the active layer for the relevant solar wavelength range of 375-750 nm is shown in Fig. 1(b). It has a photocurrent density of 10.44 mA/cm^2 based on this absorption. All gratings and nanostructures examined in subsequent sections are judged relative to this baseline photocurrent density.

#147585 - $15.00 USD Received 26 May 2011; revised 29 Jun 2011; accepted 1 Jul 2011; published 15 Sep 2011

Comparing the absorption and the AM 1.5G spectra in Fig. 1, we see that there will be substantial benefit to enhancing this cell's performance over the entire wavelength range. The benefit is particularly prominent in the 600-750 nm range where the active layer is weakly absorbing.

3. Theoretical Motivation

Based on the planar structure shown in Section 2, we seek to enhance the absorption in the active layer through light trapping. Our design is guided by a recently developed theory of nanophotonic light trapping [15]. Conventional light trapping theory was developed nearly thirty years ago, and was based on a ray optics picture appropriate for optically thick solar cells such as crystalline silicon solar cells [12]. This theory determined an upper limit for the absorption enhancement F possible due to light trapping in a solar cell as $F = 4n^2/\sin^2\theta$ where n is the refractive index of the absorbing medium, and θ is the angle of the emission cone in the medium surrounding the cell. However, when the thickness of the absorbing layer of the solar cell is as thin or thinner than the wavelength of solar light, the wave nature of the incoming radiation must be taken into account.

Recent work has shown that the conventional limit can in fact be substantially surpassed in the nanophotonic regime, where the thickness of the active layers is much smaller compared with the wavelength [13, 15]. This new nanophotonic light trapping theory provided three key pieces of guidance for this paper:

1. **Resonances**: Broadband absorption enhancement occurs due to the aggregate contributions of many optical resonances in the solar cell's active layer.

2. **Strong Coupling Regime**: Absorption is maximized when incoming solar radiation is strongly coupled to the solar cell's optical resonances. A strongly scattering layer can accomplish this, as was shown in [15].

3. **Density of State**: Enhancing the density of state in or around the active solar material increases the number of available resonances for incoming light to couple into, thereby increasing the overall capacity for absorption in the material.

In addition to these general considerations, there are challenges for light trapping that are specific to this geometry. In conventional cells, such as crystalline Si cells, the active layer, which has the highest refractive index in the layered structure, naturally forms a waveguide. Light trapping then involves scattering into the guided mode in the waveguide formed by the active layer. In the structure shown in Fig. 1(a) the active layer has an index that is, at best, comparable to that of the ITO, and is also very thin. Thus the active layer alone does not form a waveguide. Instead, the guiding layer is the ITO layer. Therefore, in this paper, we seek to achieve light trapping in the active layer, by exploiting the guided modes in the ITO layer.

4. 1D ITO Grating

We first consider a top-surface periodic dielectric grating [Fig. 2(a)] that rests on top of the usual stack of layers present in an organic solar cell: a layer of the transparent conductor PEDOT:PSS, the bulk heterojunction, a TiOx optical spacer, and a reflecting Ag back contact. The grating is introduced in the ITO layer. ITO is typically needed as a transparent front-surface contact in organic cells, and is here used as the high-index component of the top-surface grating. Structuring only the top surface allows the thin solution-processed layers of the organic solar cell to remain planar, which is experimentally desirable to prevent shorting and roughness encountered when the active layers themselves are structured.

#147585 - $15.00 USD Received 26 May 2011; revised 29 Jun 2011; accepted 1 Jul 2011; published 15 Sep 2011

4.1. *Grating Optimization*

We use RCWA to investigate the parameter space relevant to a 1D top-surface air-ITO grating. We optimize for the grating period a, the grating height h_g, the width of the ITO portion of the grating d_I and the height of the spacer layer h_s. The PEDOT:PSS layer is chosen to have a thickness of 20 nm [21] in order to optimize mode coupling to the active layer which is 35 nm in thickness.

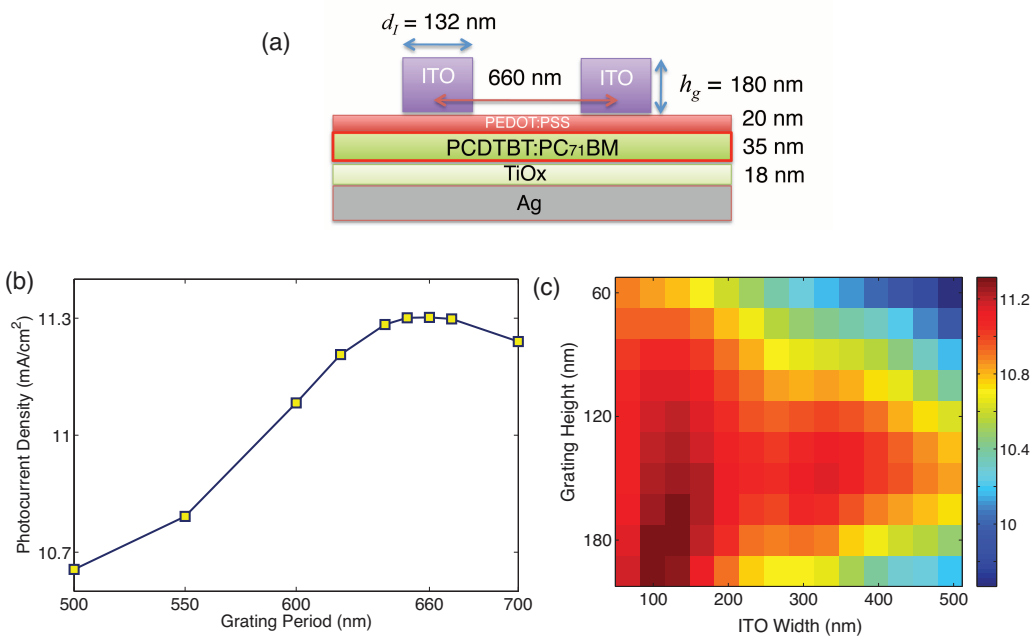

Fig. 2. (a) Diagram of the optimized 1D periodic ITO grating structure. (b) Photocurrent Density (mA/cm^2) for various grating periods, for the optimal device on other parameters, show that a 660 nm period grating is optimal for this device. (c) Photocurrent density for normally incident light as a function of ITO height and width for a grating with the optimal 660 nm period.

For a grating period of 660 nm, grating height h_g = 180 nm, ITO width d_I = 132 nm and spacer height h_s = 18 nm, we find an optimal polarization-averaged photocurrent density of 11.31 mA/cm^2. This represents a 8.31% photocurrent enhancement over the planar reference cell. The optimized structure and these parameters are illustrated in Fig. 2(a). In Fig. 2(c) we show the effect on photocurrent density of varying the grating height and ITO width while fixing the period and spacer height at their optimal points. The performance of the optimized structure is fairly robust against small fluctuations in grating period, height, and ITO width.

4.2. *Light Absorption in the Active Layer*

We now examine the absorption spectrum in the active layer of this optimized structure to understand the source of the observed photocurrent enhancement. Note here again that by absorption we mean absorption in the active PCDTBT:PC$_{71}$BM layer only; that is to say, useful absorption. In Fig. 3(a) we can see the absorption spectrum for *s*- and *p*-polarizations for the optimal grating structure, and that of the reference planar cell. For *s*-polarized light the grating

#147585 - $15.00 USD Received 26 May 2011; revised 29 Jun 2011; accepted 1 Jul 2011; published 15 Sep 2011

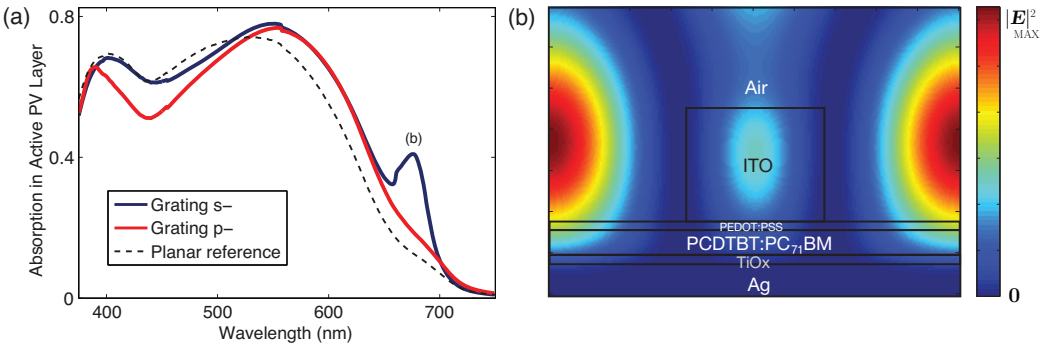

Fig. 3. (a) Absorption in the active layer for the optimal 1D ITO grating organic cell for both polarizations (solid lines) compared to the optimal planar reference cell (dashed line). The broad peak at $\lambda_0 = 677$ nm for the grating in the *s*-polarization results in significant integrated photocurrent enhancement relative to the planar cell. (b) The electric field intensity $|\mathbf{E}|^2$ at the absorption peak of $\lambda_0 = 677$ nm. The field is concentrated in the ITO layer but penetrates down into the active layer, thereby yielding useful absorption.

structure has several broad peaks including a notable peak centered at $\lambda_0 = 677$ nm with a width of $\Delta\lambda \approx 40$ nm.

The greatest contribution to the enhancement in photocurrent comes from the 677 nm peak, since this peak is both broad and located in a spectral region where the planar cell's absorption is weak. To better understand the physical origin of this peak we show the electric field intensity $|\mathbf{E}|^2$ at λ_0 in Fig. 3(b). The field is strongly concentrated in the ITO layers with its maximum lying in the air space between the higher-index ITO part of the air-ITO grating. The field penetrates into the PEDOT:PSS and active layers, thereby yielding the absorption enhancement.

The *p*-polarization spectrum shows no significant deviation from that of the planar reference cell. Thus, while the *s*-polarization has a photocurrent density of 11.75 mA/cm^2, the *p*-polarization has a photocurrent density of 10.87 mA/cm^2.

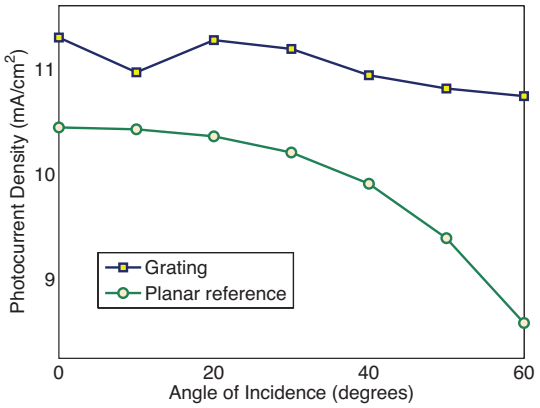

Fig. 4. Polarization-averaged photocurrent density vs. (polar) angle of incidence for planar and optimized 1D ITO grating cells. The grating structure outperforms the planar cell to large angles of incidence.

#147585 - $15.00 USD Received 26 May 2011; revised 29 Jun 2011; accepted 1 Jul 2011; published 15 Sep 2011

4.3. *Angular Response*

Finally, we calculate the angular response of the optimal structure identified earlier. In Fig. 4 we plot the photocurrent density as a function of incident (polar) angle. The polarization-averaged photocurrent density for the 1D ITO grating cell decreases with increasing angle of incidence but remains above that of the planar reference cell up to 60°, indicating substantial robustness in enhancement for a wide range of angles.

5. 2D ITO Nanostructure

A key limitation of the 1D grating is its polarization dependence [13, 22]. At the same time, it is indeed remarkable that the simple 1D grating considered in the previous section can itself deliver worthwhile polarization-averaged enhancement. In this section, to overcome the lower performance in the $p-$polarization, we examine a two-dimensional (2D) grating that is periodic in both planar dimensions. The grating structure consists of a square lattice of circular air holes in the ITO layer.

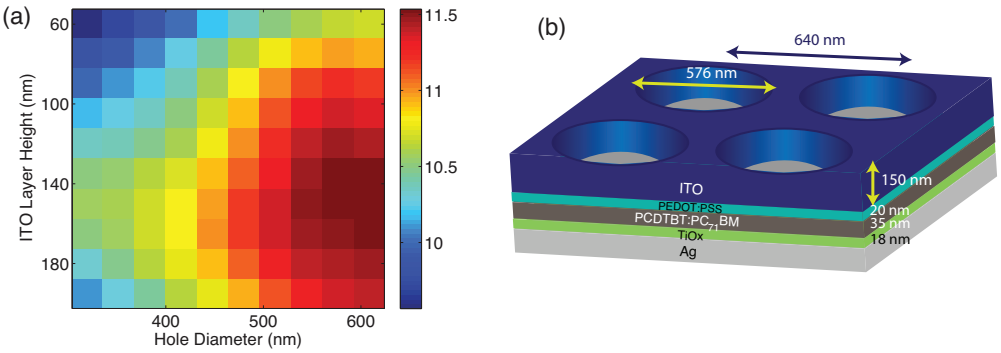

Fig. 5. (a) Photocurrent density (mA/cm^2) for normally incident light as a function of ITO nanostructure height and air hole diameter for a 640 nm period. (b) The optimized 2D ITO-air hole nanostructure on top of the organic solar cell stack.

By using circular air holes in the ITO layer the absorption spectrum becomes independent of *s*- and *p*-polarization. We optimize all tunable parameters, including the air-hole diameter and height of the ITO layer, as shown in Fig. 5(a). For a grating period of 640 nm, an air hole diameter of d_{air} = 576 nm, an ITO layer height of h_g = 150 nm and a TiOx spacer layer thickness of h_s = 18 nm, we find an optimal photocurrent density of 11.58 mA/cm^2. This is polarization-independent and represents a 10.91% photocurrent enhancement over the planar reference cell. The photocurrent achieved using this grating structure with 35 nm active layer thickness is equivalent to what can be achieved using a 41 nm thick active layer of PCDTBT:PC_{71}BM in an optimized planar cell. The optimized nanostructure is shown in Fig. 5(b).

5.1. *Absorption Spectrum*

The absorption spectrum for this optimal structure is shown in Fig. 6(a). As noted earlier, for a symmetric 2D grating the absorption spectrum is polarization-independent. There is a prominent absorption peak at λ_0 = 668 nm whose electric field intensity we show in Fig. 6(b). As can be seen the field is primarily concentrated in the air hole, with a portion of the field penetrating into the active layer thereby enhancing useful absorption.

#147585 - $15.00 USD Received 26 May 2011; revised 29 Jun 2011; accepted 1 Jul 2011; published 15 Sep 2011

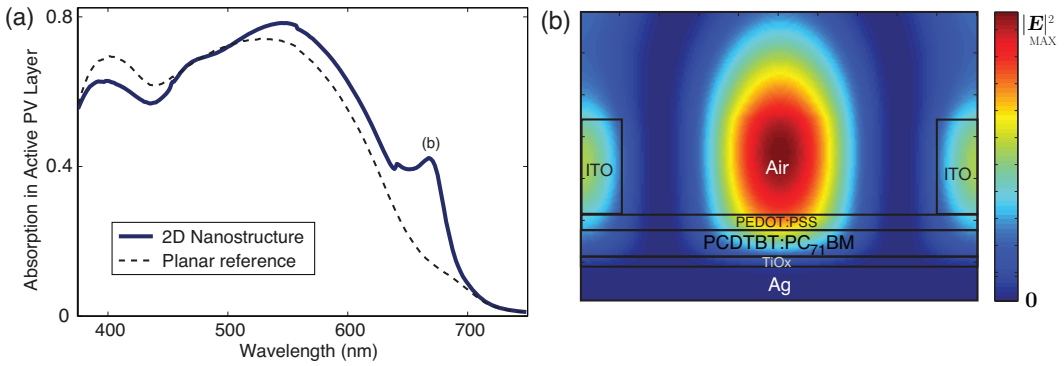

Fig. 6. (a) Absorption in the active layer comparing the 2D grating structure (solid line) against the planar reference cell (dashed line). There is a prominent peak λ_0 = 668 nm that produces notable photocurrent enhancement for both polarizations. (b) Field plot of the electric field intensity $|\mathbf{E}|^2$ at peak λ_0 = 668 nm. As with the 1D grating, the field is concentrated in the air part of the ITO layer but penetrates down into the active layer, thereby yielding useful absorption.

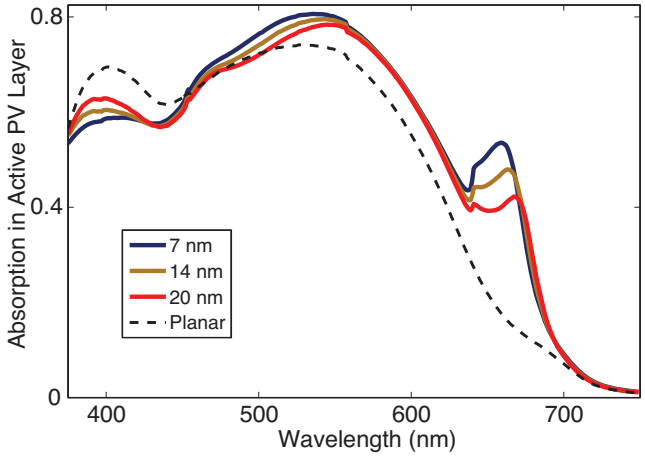

Fig. 7. Absorption spectra for optimal 2D ITO grating structures while varying the PEDOT layer height. Thinner PEDOT layers show greater absorption at the peaks.

5.2. PEDOT Layer Height

Since the absorption peak arises from a mode whose field is concentrated in the ITO layer above the organic layers, one expects that using a thinner PEDOT layer should enable more of the field to penetrate into the active layer, thereby increasing overall absorption. To test this, we fix all parameters in the optimized cell shown in Fig. 5(b), vary only the thickness of the PEDOT layer, and calculate the absorption spectrum for each case. As shown in Fig. 7, the height of the peak seen at λ_0 in the previous section increases notably with thinner PEDOT layers. The 7 nm layer in particular results in a 14.95% photocurrent enhancement relative to the planar reference cell, while the 20 nm layer results in the 10.91% photocurrent enhancement

#147585 - $15.00 USD Received 26 May 2011; revised 29 Jun 2011; accepted 1 Jul 2011; published 15 Sep 2011

noted earlier. Thus, the closer the active layer is to the grating, the stronger the enhancement.

As a practical matter, it is generally deemed necessary for the PEDOT layer to be at least 20 nm in thickness [21]. As an alternative to PEDOT however, transition metal oxides such as vanadium oxide and molybdenum oxide can be reliably deposited and used with sub-10 nm thicknesses [23,24]. While their dielectric constants are slightly higher than that of PEDOT, this does not alter the observed optical effect of the ITO mode penetrating down into the active layer. Thus, combined with the structures presented in this paper, these alternatives should enable the stronger absorption enhancement noted above.

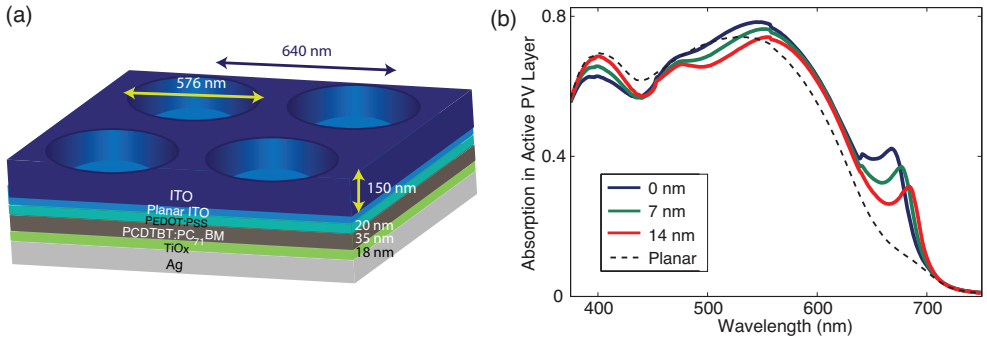

Fig. 8. (a) A thin planar ITO layer introduced below the ITO-air grating layer, as shown in this diagram, may be electrically desirable for charge carrier extraction. (b) The effect of the thickness of this planar ITO layer on light absorption in the active layer is shown for increasing thicknesses. The resonance peak's prominence decreases with increasing thickness.

5.3. Planar ITO Layer

A practical concern with the above design might be that it reduces the surface area of the ITO contact which can reduce the conductivity of the anode and increase the charge collection distance for carriers in the PEDOT layer. To alleviate this we include an additional planar layer of ITO in between the 2D ITO-air grating and the PEDOT layer, as shown in Fig. 8(a). We examine the effect of the thickness of this planar ITO layer on light absorption in the active layer in Fig. 8(b). A 7 nm planar layer of ITO reduces the photocurrent of the 2D grating device of Fig. 5(b) from 11.58 mA/cm^2 to 11.32 mA/cm^2, which still represents a 8.36% photocurrent enhancement over the planar reference cell. Moreover, combining a thin planar ITO layer with the thin metal oxide interlayer mentioned earlier, may be a practical compromise to maintaining close distance between the active and grating layers (which produces strong absorption and photocurrent enhancement), while also maintaining desirable electrical properties.

5.4. Angular Response

We also calculate the angular response of the optimal 2D structure shown in Fig. 5(b). In Fig. 9 we plot the photocurrent density as a function of incident (polar) angle. The polarization-averaged photocurrent density for the ITO grating cell decreases with increasing angle of incidence but remains well above that of the planar reference cell up to 60°.

#147585 - $15.00 USD Received 26 May 2011; revised 29 Jun 2011; accepted 1 Jul 2011; published 15 Sep 2011

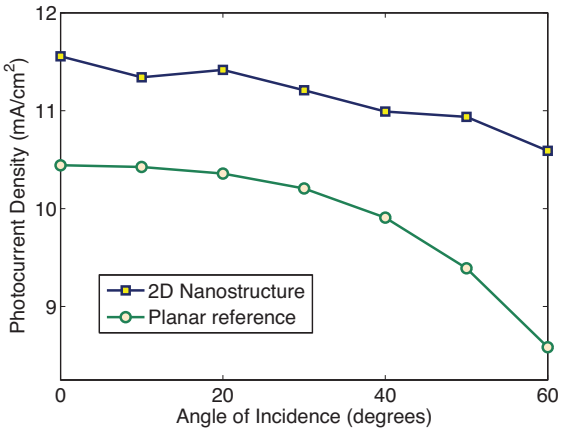

Fig. 9. Polarization-averaged photocurrent density vs. (polar) angle of incidence for planar and optimized 2D ITO nanostructure cells.

6. Multi-Level Grating

Finally, we consider more sophisticated top surface grating structures that can deliver stronger scattering than the ordered gratings considered in previous sections. One example is a multi-level grating structure, schematically shown in Fig. 10(a). This structure consists of a 2D array of ITO blocks on bottom and a 1D ITO grating on top, axially oriented at a 45° angle relative to the bottom layer.

This grating, deployed on our model system with an active layer thickness of 35 nm, results in a photocurrent of 11.49 mA/cm^2, an enhancement of 10.1% compared with the optimized planar reference cell. The photocurrent achieved using this grating structure with 35 nm active layer thickness is equivalent to what can be achieved with a 40 nm thick active layer in an optimized planar cell.

We also apply this grating structure to a cell with an active layer thickness of 70 nm. We do this to compare this multi-level grating's performance against the best PCDTBT:PC$_{71}$BM cells reported in the literature [4], where the active layer is 70-80 nm thick. When the grating structure is applied, a relatively small, yet broadband enhancement of absorption can be seen over large segments of the relevant wavelength range [Fig. 10(b)], indicating the presence of strong scattering that is not strongly wavelength dependent [15]. The 45° angle between the two grating layers is arrived at by an optimization procedure [Fig. 10(c)]. The use of this grating structure results in a photocurrent density of 14.29 mA/cm^2, a 3.1% photocurrent enhancement over the optimized 70 nm thick planar cell's photocurrent of 13.86 mA/cm^2.

We have thus shown that the use of such dielectric nanostructures can lead to enhancement in active layers with different thicknesses. This result indicates that our overall approach can be tailored to suit a variety of future bulk heterojunctions used in the active layer. Moreover, our results highlight the potential of complex, or randomly distributed, dielectric and ITO nanostructures (in particular, nanowires) to enable light absorption enhancement in the active layers of the best existing organic solar cells.

#147585 - $15.00 USD Received 26 May 2011; revised 29 Jun 2011; accepted 1 Jul 2011; published 15 Sep 2011

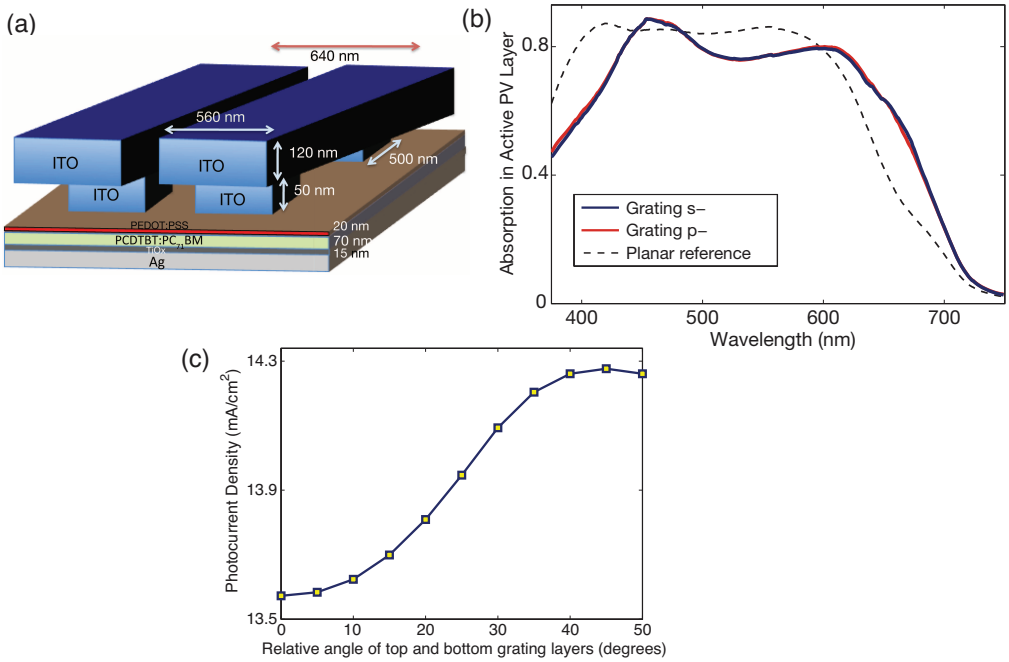

Fig. 10. (a) A multi-level grating structure consisting of a 1D ITO grating lying on top of a 2D air-ITO grating at a 45° angle relative to the bottom layer. (b) Absorption in the active layer for the multi-level grating for both polarizations compared to a planar reference cell, both with 70 nm-thick active layers [4]. (c) Photocurrent density vs. the top grating layer's angle relative to the lower layer, showing an optimum at 45°.

7. Conclusion

We have numerically demonstrated that nanostructured top-surface contacts made with ITO can significantly enhance light absorption and photocurrent generated in realistic bulk-heterojunction organic cells. Structures similar to the ITO-air gratings shown here can potentially be fabricated cheaply using electrospun ITO nanowires [25] or thermal nanoimprint lithography [26]. Thus, we believe that light absorption enhancement enabled by nanostructuring the transparent electrical contact is compatible with the low-cost manufacturing vision of organic solar cells.

More broadly, the designs presented here offer a new degree of freedom to organic photovoltaics researchers as new semiconductors are developed. By enabling partial decoupling between the issues of carrier extraction and light absorption, while allowing the active layer to remain planar, we believe such designs will prove fruitful as organic solar cells seek to go beyond 10% in efficiency.

Acknowledgments

We thank Eric T. Hoke for ellipsometry data on PCDTBT:$PC_{71}BM$. This work was supported by the Center for Advanced Molecular Photovoltaics (CAMP) (Award No KUSC1-015-21), made by King Abdullah University of Science and Technology (KAUST).

#147585 - $15.00 USD Received 26 May 2011; revised 29 Jun 2011; accepted 1 Jul 2011; published 15 Sep 2011